Available online at www.sciencedirect.com
ScienceDirect
C. R. Chimie 11 (2008) 1004–1009
COMPTES RENDUS CHIMIE
http://france.elsevier.com/direct/CRAS2C/

Full paper / Mémoire

Investigation of the electrocatalytic activity of boron-doped diamond electrodes modified with palladium or gold nanoparticles for oxygen reduction reaction in basic medium

Sabine Szunerits [a,b,*], Rabah Boukherroub [b]

[a] *Laboratoire d'électrochimie et de physicochimie des matériaux et des interfaces (LEPMI), CNRS–INPG–UJF, 1130, rue de la Piscine, BP 75, 38402 Saint-Martin-d'Hères cedex, France*
[b] *Institut de recherche interdisciplinaire (IRI, USR CNRS-3078) and électronique, de microélectronique et de nanotechnologie (IEMN), UMR CNRS 8520, Cité scientifique, avenue Poincaré, BP 60069, 59652 Villeneuve-d'Ascq, France*

Received 10 September 2007; accepted after revision 8 January 2008

Abstract

The paper reports on the electrocatalytic activity of boron-doped diamond (BDD) electrodes electrochemically modified with palladium (Pd) or gold nanoparticles (Au NPs) towards oxygen reduction reaction (ORR) in alkaline medium. The BDD/Pd NP interface shows a well-defined diffusion-controlled voltammetric oxygen reduction peak at −0.25 V vs. Ag/AgCl. This is more positive than the ORR peak at −0.59 V vs. Ag/AgCl observed on BDD/Au-NP composite electrodes. The ORR proceeds *via* a four-electron process in both cases. ***To cite this article: S. Szunerits, R. Boukherroub, C. R. Chimie 11 (2008).***

Résumé

Nous présentons nos résultats sur l'activité électrocatalytique des électrodes de diamant dopé au bore (BDD) modifiées par des nanoparticules de palladium (Pd NPs) ou d'or (Au NPs) pour la réaction de réduction d'oxygène dans le milieu alcalin. Le pic de réduction d'oxygène apparait à −0.25 V vs. Ag/AgCl pour le système BDD/Pd NPs. Il est plus positif que le pic de réduction observé à −0.59 V vs. Ag/AgCl en utilisant l'électrode BDD/Au NPs. Dans les deux cas, la réaction de réduction d'oxygène est un processus à 4 électrons. ***Pour citer cet article : S. Szunerits, R. Boukherroub, C. R. Chimie 11 (2008).***

Keywords: Boron-doped diamond electrode; Oxygen reduction; Surface termination; Palladium nanoparticles; Gold nanoparticles

Mots-clés: Électrode de diamant dopé bore ; Réduction d'oxygène ; Nanoparticles de palladium ; Nanoparticles d'or

1. Introduction

The oxygen reduction reaction (ORR) has been intensively investigated over the last years [1,2] due to its importance for fuel cell applications. A variety of

* Corresponding author. Laboratoire d'électrochimie et de physicochimie des matériaux et des interfaces (LEPMI), 1130, rue de la Piscine, BP 75, 38402 Saint-Martin-d'Hères cedex, France.
E-mail address: sabine.szunerits@lepmi.inpg.fr (S. Szunerits).

1631-0748/$ - see front matter © 2008 Académie des sciences. Published by Elsevier Masson SAS. All rights reserved.
doi:10.1016/j.crci.2008.01.015

modified and unmodified electrode materials have been suggested as cathodes for the reduction of oxygen (O_2) in different media. Electrocatalytic surfaces, consisting of nanometer-sized metallic particles of noble metals (e.g., Pt, Ru, Au, Pd) deposited onto conducting interfaces, have revealed excellent catalytic properties for ORR [3–10]. The formation of a sensitive electrocatalytic interface is based on the irreversible linking of a high density of metallic particles to the transducer, which is chemically and electrochemically stable under corrosive and oxidative conditions.

Carbon surfaces have been next to gold extensively researched as support substrates in electrocatalytic systems [11–21]. Carbon in its sp^2-hybridized form has shown excellent catalytic properties [12–17], but has shown its limitation due to its electrochemical instability, especially under oxidative conditions. With the advancement in chemical vapor deposition (CVD) techniques, boron-doped diamond (BDD) composed of sp^3 type carbon has become a highly viable alternative material. Beside its good electrical conductivity, low background current densities and a wide electrochemical potential window in aqueous electrolytes (about −1.35 V–2.3 V/NHE), BDD shows morphological stability at extreme positive and negative potentials and corrosion resistance under both acidic and alkaline conditions without any evidence of structural degradation.

ORR is though greatly inhibited on unmodified hydrogenated and oxygenated BDD surfaces compared to glassy carbon in alkaline and acidic solutions [19,22]. Research efforts were consequently aimed at irreversible linking metallic nanoparticles to BDD to obtain enhanced electrocatalysis for oxygen reduction [6,19,23,24]. We have recently demonstrated that the surface termination of BDD electrodes has a big influence on ORR [19]. In all the reported BDD composite electrodes for ORR, gold nanoparticles were used as electrocatalyst. Palladium-nanoparticle-modified BDD (BDD/Pd NP) could be an interesting alternative to BDD/Au NP interfaces. The deposition of Pd NP on diamond electrodes has been previously reported by the groups of Compton [20,21] and Chyan [18]. The BDD/Pd NP interfaces showed electrocatalytic activity towards hydrazine [20] and formaldehyde [18] and were used for the detection of protons and/or hydrogen [21]. However, Pd NP-modified BDD electrodes have not yet been investigated for the electrocatalytic reduction of oxygen. This is surprising since metallic palladium has been reported to present considerable catalytic activity for ORR in acidic electrolyte and preferentially proceeds through a four-electron pathway important for oxygen sensing [25]. Additionally, Safari et al. have recently found that high electrocatalytic effects of Pd NP arrays on carbon ionic liquid electrodes can be obtained in alkaline medium [15].

Herein, we report on our results on the electrocatalytic behavior of palladium nanoparticles modified BDD interfaces towards oxygen reduction in alkaline medium. The results are compared to BDD interfaces modified with gold nanoparticles under the same electrochemical conditions. The Pd NP-modified BDD composite electrode shows a well-defined voltammetric oxygen reduction peak at −0.25 V vs. Ag/AgCl, which is diffusion controlled and follows a four-electron process. This is more positive than the ORR peak at −0.59 V vs. Ag/AgCl observed for BDD/Au-NP composite electrodes.

2. Experimental

2.1. Materials

Palladium (II) chloride ($PdCl_2$), hydrogen tetrachloroaurate (III) trihydrate, sulfuric acid (H_2S0_4), potassium chloride (KCl), hydrochloric acid (HCl), sodium hydroxide (NaOH), potassium ferrocyanide [$Fe(CN)_6^{4-}$] were purchased from Aldrich and used without further purification.

2.2. Preparation of the diamond surfaces

Hydrogen-terminated polycrystalline boron-doped diamond layers were synthesized on a silicon high-purity p-type wafer by microwave plasma-enhanced chemical vapor deposition (PECVD) in a conventional reactor [26]. The thickness of the diamond layer is $\sim 8\ \mu m$ with a dopant concentration in the range of $\sim 10^{20}$ B atoms cm^{-3}. The film resistivity was $\leq 0.1\ \Omega\,cm$ as measured with a four-point probe.

Oxidized diamond samples were obtained through UV irradiation in air for 2 h using a low-pressure mercury arc lamp, as reported previously [27].

2.3. Electrochemical deposition of gold and palladium nanoparticles

The electrochemical formation of gold nanoparticles on the oxygen-terminated BDD surface was carried out amperometrically by applying a potential $E = 0.0$ V vs. Ag/AgCl for 60 s to the BDD interface. This corresponds to a passed charge $Q \sim -7.5 \times 10^{-3}\ C\,cm^{-2}$.

A stock solution of $PdCl_2$ (0.1 M) was prepared in HCl (3 M). The solution was heated up under stirring

until all the $PdCl_2$ was dissolved. The resulting solution was stored at room temperature. Different concentrations of $PdCl_2$ were prepared by dilution of the stock solution in appropriate quantity of aqueous KCl (0.1 M) solutions. The formation of palladium nanoparticles was achieved by electrochemical reduction of 0.5 mM $PdCl_2$ in KCl (0.1 M)/water at a potential $E = -0.2$ V vs. Ag/AgCl for 60 s. The charge passed through was $Q \sim -7.5 \times 10^{-3}$ C cm^{-2}.

2.4. Instrumentation

2.4.1. Scanning electron microscopy (SEM)

SEM images were obtained using an electron microscope ULTRA 55 (Zeiss, France) equipped with a thermal field emission emitter and three different detectors (EsB detector with filter grid, high-efficiency In-lens SE detector, Everhart–Thornley Secondary Electron Detector).

2.4.2. Electrochemical measurements

Cyclic voltammetric measurements were performed with an Autolab potentiostat 30 (Eco Chemie, Utrecht, The Netherlands). The diamond film working electrode ($A \approx 0.28$ cm^2) was sealed against the bottom of a single-compartment electrochemical cell by means of a rubber O-ring. The electrical contact was made to a copper plate through the bottom of the silicon substrate on which the diamond film was deposited. Platinum and Ag/AgCl electrodes were used as counter and reference electrodes, respectively. An aqueous solution of NaOH (0.1 M) was used for the investigation of ORR.

3. Results and discussion

3.1. Electrocatalytic behavior of unmodified BDD

Hydrogen-terminated and photochemically oxidized BDD films exhibit large overpotentials for the oxygen reduction reaction (ORR) in basic medium (0.1 M NaOH) [4,19,22,28] (Fig. 1). The oxygen reduction on H-terminated BDD displays a broad reduction peak at around $E = -1.01$ V vs. Ag/AgCl. The large overpotential for ORR recorded indicates that O_2 or the primary reaction intermediate ($O_2^{\bullet -}$) is only weakly adsorbed on H-terminated BDD. The oxygen reduction wave is even less defined on oxidized BDD and occurs inside the same potential window, as compared to other carbon materials [22]. Still, an oxidized BDD electrode exhibits a higher current density as compared to H-terminated BDD. In addition, oxidized BDD is chemically more inert than H-terminated BDD

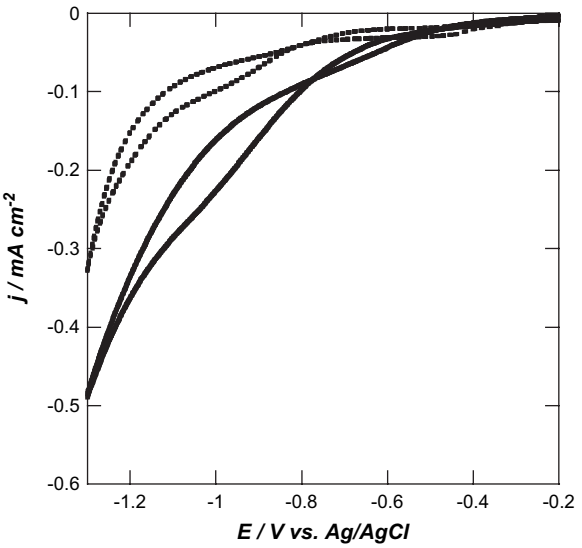

Fig. 1. Cyclic voltammograms of hydrogen-terminated (dashed line) and oxygen-terminated (full line); scan rate: 0.1 V s^{-1}.

in alkaline medium. It was also unambiguously shown by us recently that the ORR reaction mechanism in basic medium follows a direct 4-electron pathway (without formation of hydrogen peroxide intermediate), while hydrogen-terminated BDD reduces oxygen in a 2-electron process in basic conditions (Eq. (1)) [19]:

2 – electron mechanism, basic

$$O_2 + 2H_2O + 2e^- \rightleftharpoons HO_2^- + OH^- \quad (1)$$

4 – electron mechanism, basic

$$O_2 + 2H_2O + 4e^- \rightleftharpoons 4OH^- \quad (2)$$

3.2. Electrocatalytic behavior of BDD/Au NP and BDD/Pd NP

To increase the sensitivity of oxygen-terminated BDD to ORR, composite electrodes were prepared by electrochemical deposition of palladium or gold nanoparticles onto BDD. Fig. 2 displays consecutive current–potential curves obtained in aqueous solutions of 0.5 mM $NaAuCl_4$ in 0.5 M H_2SO_4 or 0.5 mM $PdCl_2$ in 0.1 M KCl on an oxygen-terminated diamond surface. Fig. 2A shows that the electrochemical reduction of $AuCl_4^-$ to metallic gold (Eq. (3)) takes place at $E_p = 0.58$ V vs. Ag/AgCl. Reversing the scan direction, a well-defined stripping response is observed at $E_p = 1.14$ V vs. Ag/AgCl. From the second cycle onwards, Au reduction appears at more positive potentials ($E_p = 0.64$ V vs. Ag/AgCl). Integration of the charge under the reduction and oxidation signals indicates

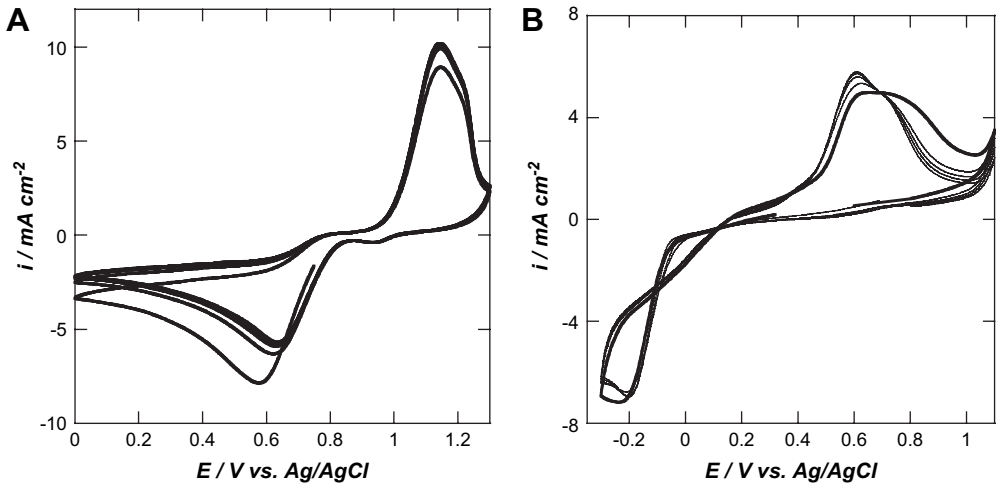

Fig. 2. Multiple scan cyclic voltammograms on oxygen-terminated BDD obtained for the reduction and re-oxidation of an aqueous solution of 0.5 mM $AuCl_4^-$/0.5 M H_2SO_4 (A) and 0.5 mM $PdCl_2$/KCl (0.1 M)/water (B); scan rate: 0.1 V s^{-1}.

that almost the same charge is consumed in both cases, leading to a stripping efficiency, $Q_{anodic}/Q_{cathodic}$ close to 1.

$$AuCl_4^- + 3e^- \rightarrow Au^0 + 4Cl^- \quad (3)$$

In the case of palladium, the electrochemical reduction starts at around 0.0 V vs. Ag/AgCl for the first scan (Eq. (4)), with a reduction peak at $E_p = -0.23$ V vs. Ag/AgCl. On reversing the potential scan, the deposited metallic palladium is voltametrically stripped at about $E_p = 0.63$ V vs. Ag/AgCl, reforming Pd^{2+}. As observed by Compton et al. [20], a cross-over is observed, indicating a nucleation and growth mechanism where the initial formation of palladium nuclei on the BDD surface serves to increase the rate of further Pd deposition. Yet again, the ratio $Q_{anodic}/Q_{cathodic}$ is almost identical, indicating a complete re-dissolution into the acidic solution.

$$PdCl_2 + 2e^- \rightarrow Pd^0 + 2Cl^- \quad (4)$$

SEM images of the obtained BDD/Au NP and BDD/Pd NP composite interfaces are shown in Fig. 3. A homogeneous distribution of nanoparticles with no preferential deposition at grain boundaries is observed in both cases, with a particle size distribution of 50–300 nm in diameter. The nanoparticle density for Au NP and Pd NP formed by passing in both cases a charge of $Q = -7.5 \times 10^{-3}$ C cm^{-2} is more than twice for BDD/Pd NP (80 Pd nanoparticles/μm^2) as compared to BDD/Au NP (35 Au nanoparticles/μm^2).

We further investigated the BDD/Au NP and BDD/Pd NP interfaces for the electrocatalytic reduction of oxygen in basic medium (Fig. 4). BDD/Au NP and BDD/Pd NP interfaces show well-defined oxygen reduction peaks in contrast to non-modified oxygen-terminated BDD. The enhanced electrocatalytic activity

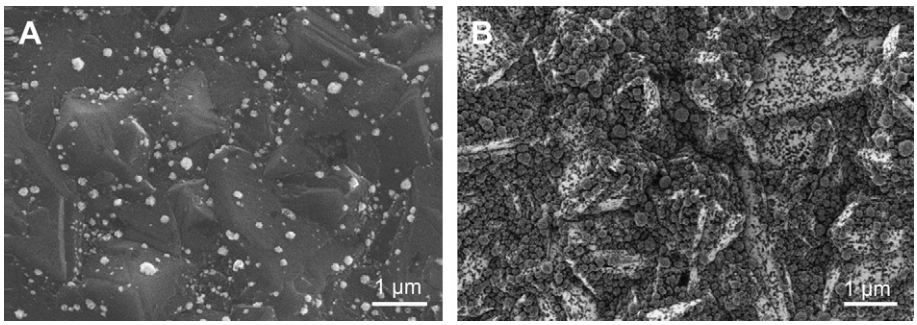

Fig. 3. SEM images of polycrystalline oxygen-terminated BDD modified with gold nanoparticles (A) and palladium nanoparticles (B); Au NP deposition conditions: 0.5 mM $AuCl_4^-$/0.5 M H_2SO_4, $E_{app} = 0$ V vs. Ag/AgCl, $Q = -2.10 \times 10^{-3}$ C; Pd NP deposition conditions: 0.5 mM $PdCl_2$/KCl (0.1 M)/water, $E_{app} = -0.2$ V vs. Ag/AgCl, $Q = -2.10 \times 10^{-3}$ C, $A = 0.28$ cm^2.

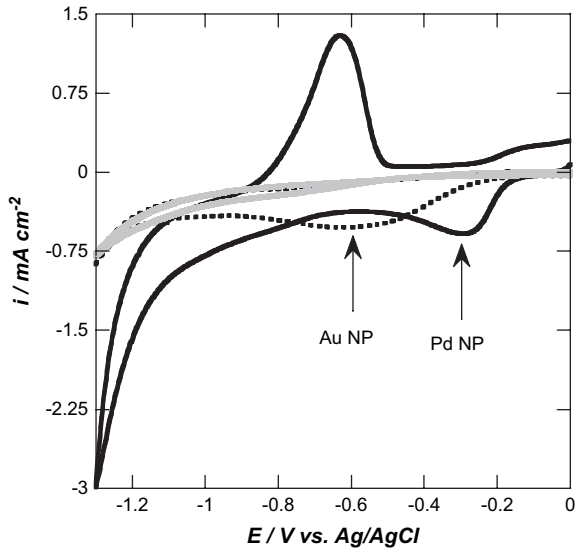

Fig. 4. Cyclic voltammograms of oxygen-terminated BDD (grey line), oxygen-terminated BDD/Au NP (black dotted line) and oxygen-terminated BDD/Pd NP (black line) in an aqueous solution of 0.1 M NaOH; scan rate: 0.1 V s^{-1}.

towards ORR is furthermore evident by the considerable shift of the oxygen reduction peak to more anodic redox potentials. For the BDD/Pd NP interface, oxygen reduction occurs at −0.25 V vs. Ag/AgCl, while for BDD/Au NP the ORR reaction is recorded at −0.59 V vs. Ag/AgCl. None of the CVs in Fig. 4 shows a cross-over, indicating that the surface state does not change during the reaction and that ORR is not changing the surface state of the composite electrodes. In addition, upon loading with NPs, the current density increased about two times in both cases (0.29 mA cm^{-2} for unmodified BDD, 0.52 mA cm^{-2} for BDD/Au NP, 0.58 mA cm^{-2} for BDD/Pd NP). The potential of ORR in basic solution using BDD/Pd NP interface is more positive than the one observed for BDD/Au NP [6,19], but about 100 mV more negative than for Au NP electrodeposited on platinum electrodes (−0.14 V vs. Ag/AgCl) [29] and Pd NP modified carbon ionic liquid electrodes (−0.185 V vs. Ag/AgCl) [15]. The difference in electrocatalytic properties of the two composite BDD electrodes could be furthermore due to the difference in deposition morphology (Fig. 3). As pointed out be El-Deab et al. [32], oxygen reduction of Au NPs deposited on carbon substrates is very sensitive to the NPs morphology. The higher Pd NPs density on BDD could be favourable for oxygen reduction catalysis.

Reversing the scan at −1.3 V vs. Ag/AgCl leads to the appearance of an oxidation peak at −0.60 V, more negative than the ORR. This is most likely due to the oxidation of H-atoms adsorbed during the negative going scan onto the palladium nanoparticles on BDD, as observed on glassy carbon [12]. When the voltammetric scan is reversed at −0.7 V vs. Ag/AgCl, this oxidation wave is not recorded.

3.3. Mechanistic considerations of BDD/Au NP and BDD/Pd NP

Rotating disk and electrochemiluminescence studies have been recently performed on BDD and BDD modified with Au NP and confirmed a 4-electron mechanism for the ORR in alkaline medium [19]. The mechanism was investigated in addition on the BDD/Pd NP interface using cyclic voltammetry [14]. Fig. 5 shows a plot of the change of the reductive peak current density of oxygen recorded on BDD/Pd NP as a function of the square root of the scan rate. A linear variation is observed demonstrating that ORR is under diffusion control on the BDD/Pd NP interface. The number of electrons (n) transferred per oxygen molecule in the electrocatalytic oxygen reduction reaction can be calculated from the slope of i_c vs. $\nu^{1/2}$ based on Eq. (5):

$$i_c = \left(2.69 \times 10^5\right) n^{3/2} A D_{O_2}^{1/2} c_{O_2} \nu^{1/2} \quad (5)$$

where c_{O_2} is the concentration of oxygen in the bulk (1.0×10^{-6} mol cm^{-3}) [30,31], D_{O_2} the diffusion coefficient of oxygen (1.9×10^{-5} cm^2 s^{-1}), A the electrode

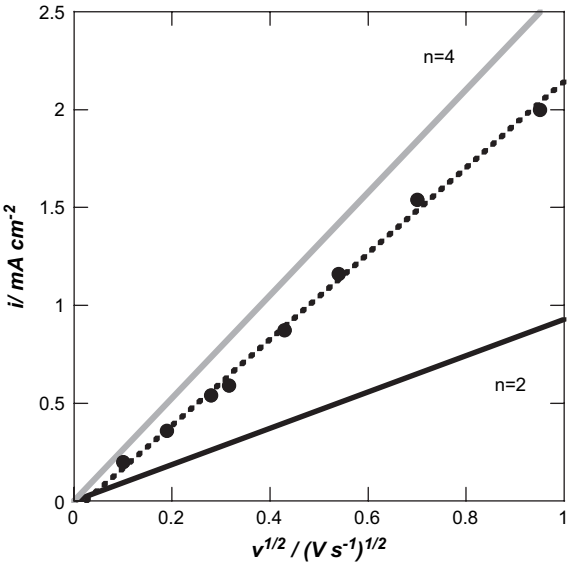

Fig. 5. Plot of oxygen reduction current vs. scan rate for BDD/Pd NP (circles) in aqueous solution of 0.1 M NaOH together with theoretical lines for $n = 2$ (black line) and $n = 4$ (grey line) obtained using Eq. (5).

area (0.28 cm^2) and ν the scan rate (0.01–0.6 $V\,s^{-1}$). Fig. 5 compares the typical responses for the theoretical and experimental i_c values against $\nu^{1/2}$ (based on Eq. (5)). The experimental values are close, in accordance with those for $n = 4$, thus supporting strongly a four-electron transfer mechanism for ORR (Eq. (2)).

4. Conclusion

The oxygen reduction reaction was investigated on BDD electrodes electrochemically modified with gold or palladium nanoparticles. BDD/Au NP and BDD/Pd NP both show enhanced electrocatalytic activity towards ORR as compared to oxygen-terminated unmodified BDD. The BDD/Pd NP interface displays a larger positive shift of the oxygen reduction potential and a slightly higher peak current density compared to the BDD/Au NP interface. This confirms once more the interest of BDD as an electrocatalytic interface, where a high density of metallic nanoparticles can be irreversibly linked. The results show the superior catalytic properties of palladium nanoparticles. The electrocatalytic activity towards other molecules, such as hydrogen peroxide, dopamine, formic acid, and ascorbic acid is under investigation in our laboratory.

Acknowledgement

The ‘‘Agence nationale de la recherche’’ (ANR), the ‘‘Centre national de la recherche scientifique’’ (CNRS) and the Nord-Pas-de Calais Region are gratefully acknowledged for financial support.

References

[1] K. Kinoshita, Electrochemical Oxygen Technology, New York, 1992.
[2] N.M. Markovic, R.R. Adzic, B.D. Cahan, E.B. Yeager, J. Electroanal. Chem. 377 (1994) 249.
[3] H. Naohara, S. Ye, K. Uosaki, Electrochim. Acta 45 (2000) 3305.
[4] T. Yano, E. Popa, D.A. Tyrk, K. Hashimoto, A. Fujishima, J. Electrochem. Soc. 146 (1999) 1081.
[5] Y. Zhang, S. Asahina, S. Yoshihara, T. Shirakashi, J. Electrochem. Soc. 48 (2003) 741.
[6] Y. Zhang, V. Suryanarayanan, I. Nakazawa, S. Yoshihara, T. Shirakashi, Electrochim. Acta 49 (2004) 5235.
[7] H. Ye, R.M. Crooks, J. Am. Chem. Soc. 127 (2005) 4930.
[8] C.M. Welch, R.G. Compton, Anal. Bioanal. Chem. 384 (2006) 601.
[9] O. Savadogo, K. Lee, K. Oishi, S. Mitsushima, N. Kamiya, K.-I. Ota, Electrochem. Commun. 6 (2004) 105.
[10] S.B. Aoun, Z. Dursun, T. Sotomura, I. Taniguchi, Electrochem. Commun. 6 (2004) 747.
[11] C.M. Welch, A.O. Simm, R.C. Compton, Electroanalysis 18 (2006) 965.
[12] V. Diculescu, A.-M. Chiorcea-Paquim, O. Corduneanu, A.M. Oliveira-Brett, J. Solid State Electrochem. 11 (2007) 887.
[13] Y. Lin, X. Cui, X. Ye, Electrochem. Commun. 7 (2005) 267.
[14] C.-C. Yang, A.S. Kumar, J.-M. Zen, Electroanalysis 18 (2006) 64.
[15] A. Safari, N. Maleki, F. Tajabadi, E. Farjami, Electrochem. Commun. 9 (2007) 1963.
[16] G. Jurmann, K. Tammeveski, J. Electroanal. Chem. 597 (2006) 119.
[17] M.S. El-Deab, T. Sotomura, T. Ohsaka, Electrochim. Acta 52 (2006) 1792.
[18] T. Arunagiri, T.D. Golden, O. Chyan, Mater. Chem. Phys. 92 (2005) 152.
[19] S. Szunerits, M. Manesse, G. Denault, B. Marcus, C. Jama, R. Boukherroub, Electrochem. Solid State Lett. 10 (2007) G43.
[20] C. Batchelor-McAuley, C.E. Banks, A.O. Simm, T.G.J. Jones, R.C. Compton, Analyst 131 (2006) 106.
[21] C. Batchelor-McAuley, C.E. Banks, A.O. Simm, T.G.J. Jones, R.C. Compton, Chem. Phys. Chem. 7 (2006) 1081.
[22] T. Yano, D.A. Tryk, K. Hashimoto, A. Fujishima, J. Electrochem. Soc. 145 (1998) 1870.
[23] Y. Zhange, S. Asahina, S. Yoshihara, T. Shirakashi, Electrochim. Acta 48 (2003) 741.
[24] A. Sarapuu, K. Tammeveski, T.T. Tenno, V. Sammelselg, K. Kontturi, D.J. Schiffrin, Electrochem. Commun. 3 (2001) 446.
[25] I.D. Burbe, J.K. Casey, J. Electrochem. Soc. 140 (1993) 1284.
[26] M. Mermoux, L. Fayette, B. Marcus, N. Rosman, L. Abello, G. Lucazeau, Diamond Relat. Mater. 4 (1995) 745.
[27] R. Boukherroub, X. Wallart, S. Szunerits, B. Marcus, P. Bouvier, M. Mermoux, Electrochem. Commun. 7 (2005) 937.
[28] J.A. Bennett, J. Wang, Y. Show, G.M. Swain, J. Electrochem. Soc. 151 (2004) E306.
[29] C.R. Raj, A.I. Abdelrahman, T. Ohsaka, Electrochem. Commun. 7 (2005) 888.
[30] A. Sarapuu, K. Helstein, D.J. Schiffrin, K. Tammeveski, Electrochem. Solid State Lett. 8 (2005) E30.
[31] R.E. Davis, G.L. Horvath, C.W. Tobias, Electrochim. Acta 12 (1967) 287.
[32] M.S. El-Deab, T. Sotomura, T. Ohsaka, J. Electrochem. Soc. 152 (2005) C730.